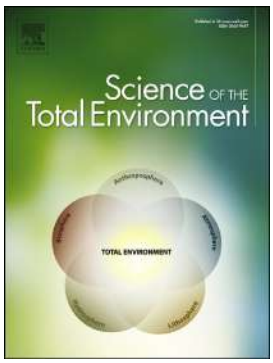

Deep learning approach for automatic microplastics counting and classification

Javier Lorenzo-Navarro, Modesto Castrillón-Santana, Elena Sánchez-Nielsen, Borja Zarco, Alicia Herrera, Ico Martínez, May Gómez

PII: S0048-9697(20)36257-4

DOI: https://doi.org/10.1016/j.scitotenv.2020.142728

Reference: STOTEN 142728

To appear in: *Science of the Total Environment*

Received date: 23 July 2020

Revised date: 15 September 2020

Accepted date: 22 September 2020

Please cite this article as: J. Lorenzo-Navarro, M. Castrillón-Santana, E. Sánchez-Nielsen, et al., Deep learning approach for automatic microplastics counting and classification, *Science of the Total Environment* (2020), https://doi.org/10.1016/j.scitotenv.2020.142728

Deep Learning Approach for Automatic Microplastics Counting and Classification

Javier Lorenzo-Navarro[a,*], Modesto Castrillón-Santana[a], Elena Sánchez-Nielsen[c], Borja Zarco[a], Alicia Herrera[b], Ico Martínez[b], May Gómez[b]

[a] *University of Las Palmas de Gran Canaria, Inst. Univ. SIANI, 35017 Las Palmas, Spain*

[b] *University of Las Palmas de Gran Canaria, Inst. Univ. ECOAQUA, 35017 Las Palmas, Spain*

[c] *University of La Laguna, Dept. Ing. Inform´ atica y Sistemas, 38271 S/C de Tenerife, Spain*

Abstract

The quantification of microplastics is a needed task to monitor its evolution and model its behavior. However, it is a time demanding task traditionally performed using expensive equipment. In this paper, an architecture based on deep learning networks is presented with the aim of automatically count and classify microplastic particles in the range of 1-5 mm from pictures taken with a digital camera or a mobile phone with a resolution of 16 million pixels or higher. The proposed architecture comprises a first stage, implemented with the U-Net neural network, in charge of making the segmentation of the particles in the image. After the different particles have been isolated, a second stage based on the VGG16 neural network classifies them into three types: fragments, pellets and lines. These three types have been selected for being the most common in the range size under consideration. The experimental evaluation was carried out using images taken with two digital cameras and one mobile phone. The particles used in experiments correspond to samples collected on the beach of Playa del Poris in Tenerife Island, Spain, (28° 09' 51" N, 16° 25' 54" W) in August 2018. A Jaccard index value of 0.8 is achieved in the experiments of particles segmentation and an accuracy of 98.11% is obtained in the classification of the microplastic particles. The proposed architecture is remarkable faster than a similar

* Corresponding author

Email address: javier.lorenzo@ulpgc.es (Javier Lorenzo-Navarro)

previously published system based on traditional computer vision techniques.

Keywords: Microplastics Classification, Image Analysis, Artificial Intelligence, Deep Learning

1. Introduction

Plastic pollution is one of the most widespread problems affecting the marine environment. Furthermore, it threatens ocean health, food safety and quality, human health, coastal tourism, and contributes to climate change (Royer et al., 2018). In 2015, Jambeck et al. (Jambeck et al., 2015) estimated that between 4.8 and 12.7 million tons of plastic end up in our seas every year. In addition to the durability of the plastic disintegration process another important issue is the fragmentation of them into smaller plastic fragments. Those classified as microplastics, smaller than 5 mm, are of great interest for the biologists because due to their reduced size they can be ingested by fishes and other marine organisms and transferred through the marine food chains (Carbery et al., 2018; Setälä et al., 2014).

[[Image]]

Figure 1: Samples of particles cropped images: (a) Pellets, (b) Fragments, (c) Lines.

In this context, the shape of the microplastic particles in the range of 1-5 mm is a cue about their origin. Thus, those originated from intentional production (primary) normally exhibit a rounded shape (Figure 1-a), while those originated from the fragmentation of larger plastics (secondary) normally exhibit irregular shapes (Figure 1-b). In addition to those microplastic particles, it is necessary to add those originated from the synthetic fabrics fibers, or lines and ropes from fishing activities (Figure 1-c).

Monitoring the amount of plastics and microplastics in the oceans involves not only to control the items that are floating in the open water, but also a large amount of them that are on the ocean floor as has been discovered recently by Kane et al. (Kane et al., 2020) due to the transport of microplastics by turbidity currents (Pohl et al., 2020). Therefore, monitoring these concentrations of microplastics in the environment has become an essential challenge to better understand their sources and sinks. In this sense, some indirect techniques have been developed to have an estimation of the amount of plastics in the ocean. One of them is based on the monitoring the plastics on the beach as they act as sentinel (Pham et al., 2020). Besides the marine

microplastics, the presence of microplastics in freshwater and terrestrial environments is also an important topic but it has not received so much attention from the research community (Wong et al., 2020). In freshwater environment, the abundance of microplastics is affected by population density and quality of waste management, and for terrestrial ecosystems the main entry points are agroecosystem, landfill and water treatment sludge.

However, one of the main problems of the quantification of plastics on the coastline is that this task is generally labor-intensive in terms of time and resources involved in collecting samples and processing them in the laboratory. In addition, most of research studies carried out to date require specific laboratory equipment such as stereo microscopes, dissecting microscopes or compound microscopes.

The use of stereo microscope for counting and sorting particles based on color, size, brightness, and morphology is the most common identification technique in sediment studies (Hanvey et al., 2017; Gauci et al., 2019) in the range of 1 - 5 mm. These parameters are widely used in the study of microplastics (Kooi and Koelmans, 2019). Consequently, the automatization of image analysis-based identification methods is an important issue when counting, classifying, and measuring some types of particles since the quantification of key figures as particle type or size requires a tedious and intensive manual labor.

One important limitation in monitoring microplastics is that their visual identification/screening process is a labor-intensive task that must be carried out by trained personnel. Therefore, it would be highly recommendable to automatize this task to result in faster sample processing and enabling this working time to be better applied to other relevant tasks. However, techniques to count and classify automatically microplastic particles with size between 1 mm and 5 mm have not been studied widely.

Lately, there has been an increasing interest in the image analysis techniques for microplastics characterization. Mukhanov et al. (Mukhanov et al., 2019) classified the microplastic particles into four classes: rounded, irregular, elongated and fiber; making use of the ImageJ software to compute three shape descriptors (Feret's diameter, circularity, and area). The same software, ImageJ, was used by Prata et al. (Prata et al., 2019) to develop the Microplastics Visual Analysis Tool (MP-VAT) whose aim was to automatically count fluorescent microplastics stained with Nile Red and specific wavelength illumination. Similarly to Mukhanov et al. (Mukhanov et al., 2019), the authors proposed the circularity of the shape to classify it as fiber,

fragment or particles, besides Feret and MinFeret diameters to give an approximation of the largest and smallest dimension of the particle.

Gauci et al. (Gauci et al., 2019) proposed the use of Matlab software to analyze the microplastic particles extracted from four beaches in Malta, computing three descriptors for each particle: size, roughness, and color. The size of the particles was estimated by fitting an ellipse and then using the major and minor axis. With respect to the roughness, it was computed as the the ratio between the difference of the particle and fitted ellipse areas and the ellipse area. Finally, the color was assigned to the closest of a set of 10 predefined colors in the RGB space.

In our previous work (Lorenzo-Navarro et al., 2020), our SMACC system was presented. This system was able to count and classify microplastics particles into five categories using as input two images acquired with a high resolution flat scanner. Previously to the classification process, an adaptive thresholding was carried out and each detected particle was classified using a cascade classifier achieving 91.1% of accuracy.

In recent years, deep learning approaches have gained increasing attention due to their very good performance in many computer vision tasks (Liu et al., 2020). To our best knowledge, the only application of deep learning to microplastics analysis has been the work of Wegmayr et al. (Wegmayr et al., 2020) to segment microplastics fibers in microscopy images. In their work, the authors compared the performance of Mask-RCNN (He et al., 2017) and Deep Pixel Embeddings (De Brabandere and Davy Neven, 2017), and they obtained the best results with the latter combined with a heuristic for fiber merging in the intersections.

All the previous methods based on image analysis have required dedicated equipment as special staining dyes and light (Prata et al., 2019), flat scanner (Mukhanov et al., 2019) (Gauci et al., 2019) (Lorenzo-Navarro et al., 2020) or microscopy images (Wegmayr et al., 2020). The methodology proposed in this work is based on images taken with cameras or mobile phones with a resolution of at least 16 million pixels. Furthermore, introducing deep learning techniques improves both the performance of traditional computer vision methods and even the use of manual classification, which is error-prone due to its repetitive and tedious nature. Though deep learning architectures are best suited to be deployed in graphics processing unit (GPU) based computers, the proposed methodology is fast enough even when running in computers without GPU.

Thus, the aim of this work is to present a novel method for automatizing the processes of counting and classifying microplastic particles using non-specific laboratory equipment. The main

contributions of the paper can be summarized as: 1) the use of novel techniques based on deep learning for this problem, 2) the possibility of using an image of the sample acquired with a digital camera or mobile phone without any requirement on the use of specific laboratory equipment, and 3) reduce the processing time, enabling fast results in comparison to traditional methods.

2. Methodology

Microplastics classification from an image is included in the broad category of object detection problem (Liu et al., 2020). When detecting an object in an image, it can be obtained its bounding-box that allows locating it in the image. Some of the most referenced bounding-box based deep architectures are R-CNN (Girshick et al., 2014), Fast R-CNN (Girshick, 2015), (Ren et al., 2015), YOLO (Redmon et al., 2016) and SSD (Liu et al., 2016). These methods are adequate in applications where it is enough to know where and how many times an object appears in the image. In the context of microplastics classification, it is essential to obtain the pixels of the particle to estimate the size. In this case, object instance segmentation architectures are more suitable because they do not only detect the object but they also label each pixel with the class of its enclosing object. Some deep network architectures for object instance segmentation are FCNN (Long et al., 2015), Mask-RCNN (He et al., 2017), and U-Net (Ronneberger et al., 2015).

[[Image]]

Figure 2: General schematic view of the proposed architecture.

The method presented in this work is a hybrid approach between a bounding-box based approach and an instance segmentation approach (Figure 2). Thus the proposal is divided into two sequential phases: microplastics segmentation and microplastics classification. In the first phase, an instance segmentation is realized to detect the particles in the sample image encompassing all the types of microplastics in only one, the class *particle* versus the background. As result of this first phase, the pixels that correspond to particles in the images are obtained and not only the bounding box. This result is important in microplastics analysis because as it was mentioned in the introduction, the shape of the particles is a cue about its origin. After the microplatics has been segmented in the sample image, in the second phase, each particle is classified with a fine-tuned convolutional neural network (CNN). According to the research work proposed by (Hartmann et

al., 2019), most of the microplastic particles (larger than 1 mm) can be classified into three different types based on their shape: pellets, fragments and lines. Pellets correspond to small beads of primary microplastics (Figure 1-a). Fragments correspond to small fragments derived from the breakdown of larger plastic debris (Figure 1-b). Lines correspond to small segments of fish lines or nets (Figure 1-c). There are two main reasons why the hybrid architecture is proposed instead of using an existing instance segmentation neural network. Firstly, the number of trainable parameters of those models is very high, for example, Mask-RCNN with 1024x1024 input size and a ResNet101 backbone with pre-trained weights, has 21,069,086 trainable parameters. Thus, the number of images necessary to train the network must be in the order of several thousands. Given the fact that annotation of microplastics images is a very time consuming task for expert researchers, it is very hard to have available so many training images. On the other hand, even by having enough training images, microplastic particle size (1-5 mm) requires using relatively high resolution images (16 megapixels and higher) to keep smallest particles visible. Therefore, if the image size is reduced to fit with the input size of object instance segmentation networks (1024x1024 or lower), some small microplastic particles can be blurred and even disappear.

2.0.1. Microplastics Image Segmentation

The first phase of instance segmentation is carried out with a U-Net network (Ronneberger et al., 2015) that was originally proposed for biomedical image segmentation at pixel level. This network has the advantage over other architectures that it requires a reduced number of images to train it successfully. The architecture is made up of two paths: one contracting path that is composed of convolutions layers, and the expansive path that is composed of up-convolutions. A characteristic of this architecture is the concatenation of features from the contracting path to those of the expansive path.

[[Image]]

Figure 3: Division of the sample image into 512x512 pixels patches. (solid red line: non-overlapped patches, dashed green line: overlapped patches)

As stated previously, the resolution of the samples images must be high enough to keep the details of small particles so they can not be downsized to feed the network. The solution was to

divide the sample image into smaller overlapped patches (Figure 3), apply the instance segmentation to each patch, and finally concatenate the patches to reconstruct the resulting segmented sample image. Using overlapped patches instead of non-overlapped ones is a way to solve the evident drawback of considering a single particle as two different ones when it fall between two adjacent non-overlapped patches. In our proposal, the images to be segmented are divided into 512x512 pixels patches with a horizontal and vertical stride of 256 pixels, therefore in the reconstruction of the segmented image the patches are concatenated with an overlapping as can be seen in Figure 4.

[[Image]]

Figure 4: Microplastics segmentation with overlapped patches to avoid breaking a particle in two adjacent patches.

2.1. Microplastics Classification

Once the microplastic particles have been segmented, the VGG16 network (Simonyan and Zisserman, 2015) classifies each particle into one of the three classes under consideration. VGG16 is a CNN whose architecture is composed by two blocks of two convolutional layers followed by a max-pool layer, three blocks of three convolutional layers followed by a max-pool layer, and three fully-connected layers. All the convolutional layers have a Rectified Linear Unit (ReLU) activation function.

Some modifications have been introduced into the original VGG16 architecture to adapt it to the microplastics classification task. Firstly, the dimension of the input images has been set to 132x132 pixels in RGB color instead of the original 224x224 pixels. From the three fully-connected layers, the two first ones have been reduced to 128 and 64 units respectively, and a batch normalization layer (Ioffe and Szegedy, 2015) is introduced after each layer. The last layer has three outputs, corresponding to the microplastic classes under consideration, with a softmax activation function. To reduce the number of samples necessary in the training process, the convolutional layers of the network are initiliazed with weights that had been pre-trained on ImageNet.

3. Experiments and Results

The experiments have been carried out with particles obtained from real samples collected in the beach of Playa de Poris in the island of Tenerife (28° 09' 51" N, 16° 25' 54" W). The sampling campaign took place in August, 2018.

3.1. Microplastics Segmentation Results

To assess the performance of each of the two phases of the proposed architecture, two experiments have been carried out. First, to train and test the U-Net, 49 images of mixed microplastics samples (Figure 3 left) were acquired with an Olympus OM-D EM-10 camera (26 images of 4608x3456 pixels) and with a Samsung A5 mobile phone (23 images 4608x2592 pixels), over a white background (DIN-A4 paper). Both the camera and the mobile phone configurations were set to default (autofocus and automatic whitebalance). The images where taken with indoor laboratory illumination conditions. The laboratory has 12 8W led tubes that provide an uniform light level of 500 lux aprox. The images were divided into 512x512 pixels patches as explained above, and 240 patches (120 of each camera) were randomly chosen from a total of 1484 patches. The true segmentation of these 240 patches was obtained by manually annotating the regions occupied by the particles (Figure 5 (b)).

[[Image]]

Figure 5: (a) Samples of patches, (b) Manual annotation, (c) U-Net segmentation, (d) Sauvola segmentation.

With the 240 annotated patches, a 5-fold cross validation experimental setup and four quality measures are considered:

- Accuracy is the number of pixels correctly classified as particle and non-particle.
- Precision is the ratio between correct classified pixels as particle, and the number of correct classified pixels as particle plus the number of pixels incorrectly classified as particle. The precision is intuitively the ability of the segmenter not to label as particle a pixel that is background.
- Recall is the ratio between correct classified pixels as particle, and the number of correct classified pixels as particle plus the number of pixels incorrectly classified as non-particle. The recall is intuitively the ability of the segmenter to find all the pixels

corresponding to particles.

- Jaccard index, also known as Intersection-of-Union, is defined as the number of correct classified pixels divided by the number of pixels of the union of the ground truth and the classified pixels.

Table 1: Results for microplastics segmentation with U-Net.

[[Image]]

Table 1 shows the results for the five folds and the average. It can be observed that the accuracy is very high but this measure is not informative in very unbalanced problems as this case, where the number of non-particles pixels in the image is much higher than particles pixels. Better conclusions can be obtained with precision and recall. In both cases the values are high demonstrating the ability of U-Net to segment correctly the particles in the patches. This behavior is confirmed with the value of the Jaccard index that is considered a good value when it is over 0.70 (Lin et al., 2014) and in our experiments a value of 0.80 is reached. Some results of the particles segmentation can be seen in Figure 5 (c).

In recent published works on microplastics classification based on image analysis, as those proposed by Lorenzo-Navarro et al. (Lorenzo-Navarro et al., 2020) and Wegmayr et al. (Wegmayr et al., 2020), Sauvola adaptive thresholding (Sauvola and Pietikäinen, 2000) has been applied. In order to compare the results of U-Net, the patches were segmented using the Sauvola method and the average accuracy, precision and recall was 96.39%, 71.16% and 48.37% respectively. Though the accuracy is high, as stated previously, this measure is not informative in unbalanced problems. Precision has a good value that can be interpreted that Sauvola method does not detect false particle pixels, but the low value of recall means that many particle pixels are not detected by the method. As shown in Figure 5 (d), the low recall value may be due to the light colored particles that are very common because they become discolored for the ultraviolet rays.

3.2. Microplastics Classification Results

To evaluate the performance of the second phase of this research, an expert provided us with two samples of each of the three type of microplastics under consideration. A photo of each sample was taken with two different cameras, an Olympus OM-D EM-10 and a Sony α 6400 over

a white background (DIN-A4 paper) and indoor laboratory illumination (led tubes). Each image was segmented and the cropped image of each particle was extracted (Figure 1). The number of extracted particle images was 583: 169 fragments, 204 lines and 210 pellets.

A 5-fold cross-validation experimental setup was used, and to increase the number of training samples a data augmentation process was introduced, entailing the rotation of each particle cropped image by $\pi/4$, $\pi/2$ and $3\pi/4$ clockwise, and using both the original and its mirrored cropped image, multiplying by 8 the number of training samples. A fine tuning of the pre-trained VGG16 with Imagenet was implemented with SGD optimizer (learning rate = 10^{-5}, decay = 10^{-6}, momentum = 0.9, and batch size = 16) and using 20% of the training samples as validation. In order to determine the number of epochs and to avoid overfitting, an early stopping strategy was used with a patience of 10 epochs, which means that if during 10 epochs the validation loss does not improve, then the training is stopped.

Table 2: Results for microplastics classification with VGG16 network.

[[Image]]

The accuracy and other performance measures are shown in Table 2. It can be observed that the 5-fold average accuracy is 98.11%, and the precision and recall are very similar to the accuracy which means that the behavior is similar in all classes. It can be highlighted that the number of epochs to get these results are very few. The best results without overfitting are obtained with an average of 26 epochs. Analyzing the errors, it is observed that only some pellet particles are incorrectly classified as fragment particles, but not in a noteworthy number. In Figure 6, it can be observed some examples of the misclassified particles. The fragment particle that is incorrectly classified as pellet, shows a rounded uniform shape that is more likely to occur in pellets than in other types. In the case of the misclassified pellets particles, they present an irregular shape, which is a common feature in fragment particles.

[[Image]]

Figure 6: Examples of misclassified particles.

A drawback of deep learning approaches is the need of GPUs to speed up the

computations. To test the influence of the use of GPU in the processing time, the images of the six samples (two of each microplastic type) were processed with the proposal architecture shown in Figure 2. The average time to process the images in a computer with a microprocessor (CPU) Intel Xeon 4110 was 23.87 secs. while this average time was reduced to 7.02 secs. when the computer is equipped with a GPU NVidia GeForce GTX 1080Ti. It can be observed that the processing time with the CPU is three times longer than using a GPU but in no case this is an excessive time compared to human classification.

4. Discussion

The results obtained with the proposed architecture have shown that the automatic classification of 1-5 mm microplastics can be carried out without any specific equipment such as high resolution flat scanner or microscope. Thus, in this work the experiments have been performed with mid-range digital cameras and mobile phones and the results are very promising to keep validating the approach in real quantification campaigns. Unlike bounding-box object detection networks where the object of interest is expected to have a size ratio with respect to the image (for example the Region Proposal Network (RPN) in Fast-RCNN (Girshick, 2015)), the proposed hybrid approach exhibits a higher scale invariance due to the fact that the segmentation and classification phases are decoupled. Therefore, it can be applied in other plastic shape classification problems, not only microplastics one but larger particles, up to 50 mm. In Figure 7, the classification of large fragments and lines is shown, where most of the pieces are correctly classified as fragments (Fig. 7-a) and lines (Fig. 7-b) respectively.

[[Image]]

Figure 7: Classification results of non-microplastics (larger than 5 mm) samples: (a) Fragments and (b) Lines.

The use of images taken with digital photo cameras or mobile phones has not implied that the processing time were longer than with other work using specific equipment. In a previous work (Lorenzo-Navarro et al., 2020) where SMACC system is presented, a comparison of manual versus automatic classification time is shown. In Table 3, a comparison with the proposed approach is provided. Without loss of generality, we can assume that the preparation and removal

times are the same when scanning a sample and when taking a picture. With respect to the image acquisition, it has been considered the time needed to download the images from the camera or mobile phone to the computer. It can be seen that the average processing time of one image of a microplastic sample has been reduced to the half respect to SMACC, but if the preparation and removal time are not considered it can be seen that the reduction is even larger. Thus, if only acquisition and processing time are accounted, the reduction is from 6:15 minutes with SMACC to 0:52 minutes and 1:08 minutes with the current proposal with and without GPU, respectively. Although all the experiments have been carried out with samples obtained from marine environment (beaches), the approach can be applied in other ecosystems as freshwater and terrestrial. The only requirement is to preprocess the samples to remove non-plastic materials as organic or sand.

Table 3: Average time in minutes of the whole procedure for a microplastic sample classification. *Manual* and *SMACC* times correspond to those reported in (Lorenzo-Navarro et al., 2020).

[[Image]]

As any image analysis technique, the method described in this work is influenced by the illumination conditions. In this sense, the use of images taken outdoor with sunlight or cloudy conditions probably will produce not satisfactory results. Although it could seem a limitation of the proposed method, it must be noted that previously to count and classify the particles, a cleaning process must be done in the laboratory to remove non-plastics material of the samples (Herrera et al., 2018). Therefore, considering that the researchers need to process the sample in the laboratory, indoor illumination conditions are going to be the most frequent one. On the other hand, though only white color for the background has been tested, it must not affect the performance whenever the neural networks, U-Net and VGG16, were trained with images taken with a different background color.

In summary, it can be concluded that the use of deep learning architectures for classifying microplastic samples from images taken with no specific acquisition equipment yields promising results, comparable and even with high accuracy than other proposed works based on traditional computer vision techniques, or even manual inspection. With respect to the processing time, the proposed architecture processes a sample image in a few seconds even in a computer with no GPU,

and faster if a GPU is used. In both cases, the processing time is significantly lower than previous systems based on traditional computer vision techniques.

Acknowledgments

This work was supported in part by the projects MICROTROFIC (ULPGC2015-04), financed by the University of Las Palmas de Gran Canaria, IMPLAMAC (MAC2/1.1a/265) financed by the Interreg MAC (European Fund to Regional Development, Macaronesian Cooperation), and TIN2016-78919-R, PID2019-107228RB-I00 and GOB-ESP2019-03 financed by the Spanish Ministry of Science and Innovation.

References

Carbery, M., O'Connor, W., Thavamani, P., 2018. Trophic transfer of microplastics and mixed contaminants in the marine food web and implications for human health. Environment International 115, 400–409.

De Brabandere, B., Davy Neven, L.V., 2017. Semantic instance segmentation for autonomous driving, in: The IEEE Conference on Computer Vision and Pattern Recognition (CVPR) Workshops, pp. 7–9.

Gauci, A., Deidun, A., Montebello, J., Abela, J., Galgani, F., 2019. Automating the characterisation of beach microplastics through the application of image analyses. Ocean & Coastal Management 182, 104950. doi: https://doi.org/10.1016/j.ocecoaman.2019.104950.

Girshick, R., 2015. Fast r-cnn, in: 2015 IEEE International Conference on Computer Vision (ICCV), pp. 1440–1448.

Girshick, R., Donahue, J., Darrell, T., Malik, J., 2014. Rich feature hierarchies for accurate object detection and semantic segmentation, in: 2014 IEEE Conference on Computer Vision and Pattern Recognition, pp. 580–587.

Hanvey, J.S., Lewis, P.J., Lavers, J.L., Crosbie, N.D., Pozo, K., Clarke, B.O., 2017. A review of analytical techniques for quantifying microplastics in sediments. Anal. Methods 9, 1369–1383. doi: 10.1039/C6AY02707E.

Hartmann, N.B., Hüffer, T., Thompson, R.C., Hassellöv, M., Verschoor, A., Daugaard, A.E., Rist, S., Karlsson, T., Brennholt, N., Cole, M., Herrling, M.P., Hess, M.C., Ivleva, N.P., Lusher,

A.L., Wagner, M., 2019. Are we speaking the same language? recommendations for a definition and categorization framework for plastic debris. Environmental Science & Technology 53, 1039–1047. doi: 10.1021/acs.est.8b05297.

He, K., Gkioxari, G., Dollár, P., Girshick, R., 2017. Mask r-cnn, in: 2017 IEEE International Conference on Computer Vision (ICCV), pp. 2980–2988.

Herrera, A., Garrido-Amador, P., Martínez, I., Samper, M.D., López-Martínez, J., Gómez, M., Packard, T.T., 2018. Novel methodology to isolate microplastics from vegetal-rich samples. Marine Pollution Bulletin 129, 61–69.

Ioffe, S., Szegedy, C., 2015. Batch normalization: Accelerating deep network training by reducing internal covariate shift, in: Bach, F., Blei, D. (Eds.), Proceedings of the 32nd International Conference on Machine Learning, PMLR, Lille, France. pp. 448–456.

Jambeck, J.R., Geyer, R., Wilcox, C., Siegler, T.R., Perryman, M., Andrady, A., Narayan, R., Law, K.L., 2015. Plastic waste inputs from land into the ocean. Science 347, 768–771. doi: 10.1126/science.1260352.

Kane, I.A., Clare, M.A., Miramontes, E., Wogelius, R., Rothwell, J.J., Garreau, P., Pohl, F., 2020. Seafloor microplastic hotspots controlled by deep-sea circulation. Science doi: 10.1126/science.aba5899.

Kooi, M., Koelmans, A.A., 2019. Simplifying microplastic via continuous probability distributions for size, shape, and density. Environmental Science & Technology Letters 6, 551–557. doi: 10.1021/acs.estlett.9b00379.

Lin, T.Y., Maire, M., Belongie, S., Hays, J., Perona, P., Ramanan, D., Dollár, P., Zitnick, C.L., 2014. Microsoft coco: Common objects in context, in: Fleet, D., Pajdla, T., Schiele, B., Tuytelaars, T. (Eds.), Computer Vision – ECCV 2014, Springer International Publishing, Cham. pp. 740–755.

Liu, L., Ouyang, W., Wang, X., Fieguth, P., Chen, J., Liu, X., Pietikäinen, M., 2020. Deep learning for generic object detection: A survey. International Journal of Computer Vision 128, 261–318. doi: 10.1007/s11263-019-01247-4.

Liu, W., Anguelov, D., Erhan, D., Szegedy, C., Reed, S.E., Fu, C., Berg, A.C., 2016. SSD: single shot multibox detector, in: Leibe, B., Matas, J., Sebe, N., Welling, M. (Eds.), 14th European Conference on Computer Vision (ECCV), Springer, Amsterdam, The Netherlands. pp. 21–37. doi: 10.1007/978-3-319-46448-0_2.

Long, J., Shelhamer, E., Darrell, T., 2015. Fully convolutional networks for semantic segmentation, in: IEEE Conference on Computer Vision and Pattern Recognition (CVPR), pp. 3431–3440.

Lorenzo-Navarro, J., Castrillón-Santana, M., Santesarti, E., De Marsico, M., Martínez, I., Raymond, E., Gómez, M., Herrera, A., 2020. SMACC: A system for microplastics automatic counting and classification. IEEE Access 8, 25249–25261. doi: 10.1109/ACCESS.2020.2970498.

Mukhanov, V.S., Litvinyuk, D.A., Sakhon, E.G., Bagaev, A.V., Veerasingam, S., Venkatachalapathy, R., 2019. A new method for analyzing microplastic particle size distribution in marine environmental samples. Ecologica Montenegrina 23, 77–86.

Pham, C.K., Pereira, J.M., Frias, J.P.G.L., Ríos, N., Carriço, P., Juliano, M., Rodríguez, Y., 2020. Beaches of the azores archipelago as transitory repositories for small plastic fragments floating in the north-east atlantic. Environmental pollution 263.

Pohl, F., Eggenhuisen, J.T., Kane, I.A., Clare, M.A., 2020. Transport and burial of microplastics in deep-marine sediments by turbidity currents. Environmental Science & Technology 54, 4180–4189. doi: 10.1021/acs.est.9b07527.

Prata, J.C., Reis, V., Matos, J.T.V., da Costa, J.P., Duarte, A.C., Rocha-Santos, T., 2019. A new approach for routine quantification of microplastics using nile red and automated software (mp-vat). Science of the total environment 690, 1277â€”1283. doi: 10.1016/j.scitotenv.2019.07.069.

Redmon, J., Divvala, S.K., Girshick, R.B., Farhadi, A., 2016. You only look once: Unified, real-time object detection, in: 2016 IEEE Conference on Computer Vision and Pattern Recognition, CVPR, Las Vegas, NV, USA. pp. 779–788. doi: 10.1109/CVPR.2016.91.

Ren, S., He, K., Girshick, R., Sun, J., 2015. Faster r-cnn: Towards real-time object detection with region proposal networks, in: Cortes, C., Lawrence, N.D., Lee, D.D., Sugiyama, M., Garnett, R. (Eds.), Advances in Neural Information Processing Systems 28. Curran Associates, Inc., pp. 91–99.

Ronneberger, O., Fischer, P., Brox, T., 2015. U-net: Convolutional networks for biomedical image segmentation, in: Navab, N., Hornegger, J., Wells, W.M., Frangi, A.F. (Eds.), Medical Image Computing and Computer-Assisted Intervention (MICCAI 2015), pp. 234–241.

Royer, S.J., Ferrón, S., Wilson, S.T., Karl, D.M., 2018. Production of methane and ethylene from

plastic in the environment. PLoS One 13. doi: 10.1371/journal.pone.0200574. 1 August 2018.

Sauvola, J., Pietikäinen, M., 2000. Adaptive document image binarization. Pattern Recognition 33, 225–236.

Setälä, O., Fleming-Lehtinen, V., Lehtiniemi, M., 2014. Ingestion and transfer of microplastics in the planktonic food web. Environmental Pollution 185, 77 – 83. doi: https://doi.org/10.1016/j.envpol.2013.10.013.

Simonyan, K., Zisserman, A., 2015. Very deep convolutional networks for large-scale image recognition, in: Bengio, Y., LeCun, Y. (Eds.), 3rd International Conference on Learning Representations, ICLR. Conference Track Proceedings.

Wegmayr, V., Sahin, A., Sæmundsson, B., Buhmann, J.M., 2020. Instance segmentation for the quantification of microplastic fiber images, in: Proceedings of the 2020 Winter Conference on Applications of Computer Vision (WACV '20), USA. pp. 2199–2206.

Wong, J.K.H., Lee, K.K., Tang, K.H.D., Yap, P.S., 2020. Microplastics in the freshwater and terrestrial environments: Prevalence, fates, impacts and sustainable solutions. Science of The Total Environment 719, 137512. doi: 10.1016/j.scitotenv.2020.137512.

Credit author statement

Javier Lorenzo-Navarro: Conceptualization, Methodology, Software,Writing
Modesto Castrillon-Santana: Conceptualization, Writing
Elena Sanchez-Nielsen: Conceptualization, Writing
Borja Zarco: Software
Alicia Herrera: Methodology, Writing - Review and Editing
Ico Martinez: Methodology, Resources
May Gomez: Methodology, Writing - Review and Editing
1

Declaration of interests

☒ The authors declare that they have no known competing financial interests or personal relationships that could have appeared to influence the work reported in this paper.

☐The authors declare the following financial interests/personal relationships which may be considered as potential competing interests:

Table 1

Fold	Accuracy	Precision	Recall	Jaccard Index
1	99.31%	90.98%	94.46%	0.82
2	99.14%	88.72%	96.69%	0.84
3	98.95%	86.40%	98.17%	0.79
4	97.45%	82.70%	96.14%	0.74
5	99.26%	91.12%	94.78%	0.82
Average	**98.82±0.78%**	**87.98±3.73%**	**96.05±1.50%**	**0.80±0.04**

Table 2

Fold	Accuracy	Precision	Recall	Num. epochs
1	98.26%	98.35%	98.26%	38
2	97.50%	97.57%	97.50%	22
3	95.58%	95.70%	95.58%	20
4	100.0%	100.0%	100.0%	36
5	99.19%	99.21%	99.19%	14
Average	**98.11±1.70%**	**98.17±1.65%**	**98.11±1.70%**	**26±10.49**

Table 3

Method	Preparation	Image acquisition	Classification	Remove simple	Total
Manual	00:32	-	20:24	01:32	22:28
SMACC	02:53	05:40	00:35	00:45	09:53
Ours (CPU)	02:53	00:45	00:23	00:45	04:46
Ours (GPU)	02:53	00:45	00:07	00:45	04:30

Highlights

- Novel microplastic classi_cation model based on deep learning
- Image acquisition with digital camera or mobile phone
- High classi_cation accuracy rates on common particles types

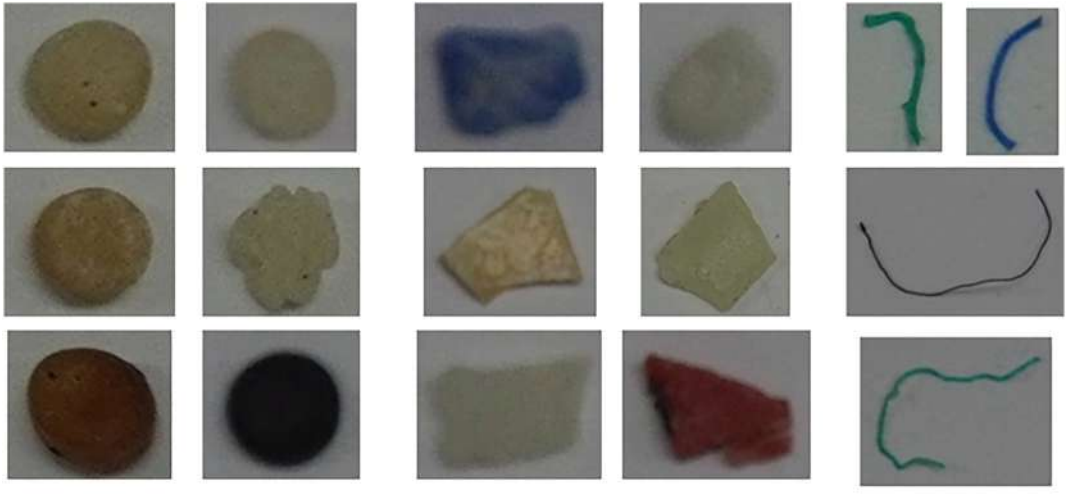

Figure 1

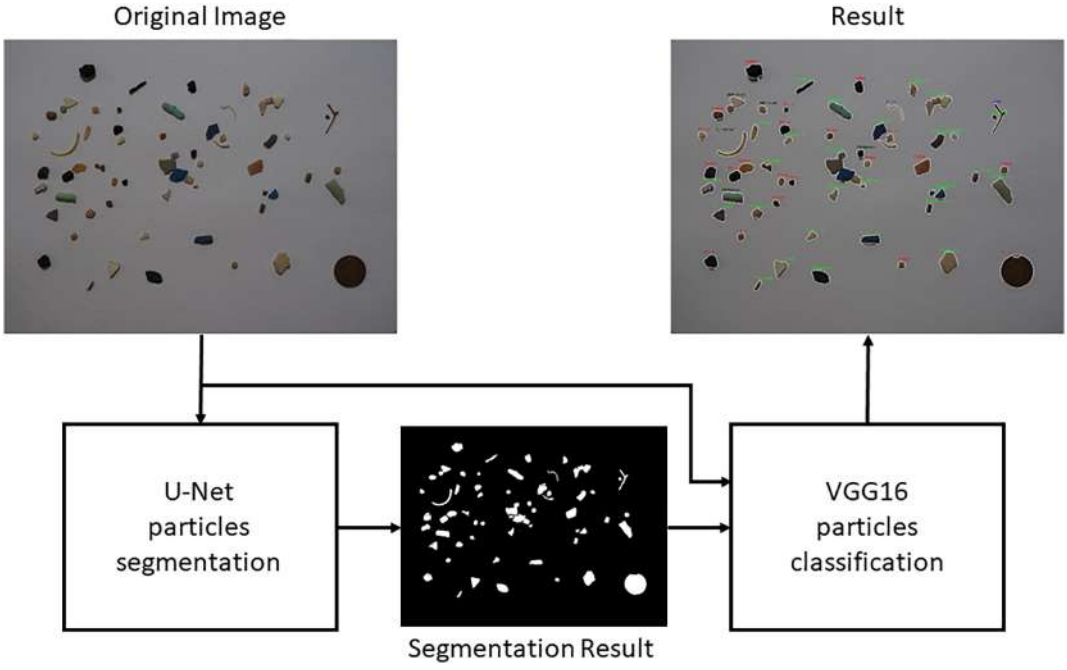
Original Image
Result
U-Net
particles
segmentation
Segmentation Result
VGG16
particles
classification

Figure 2

Figure 3

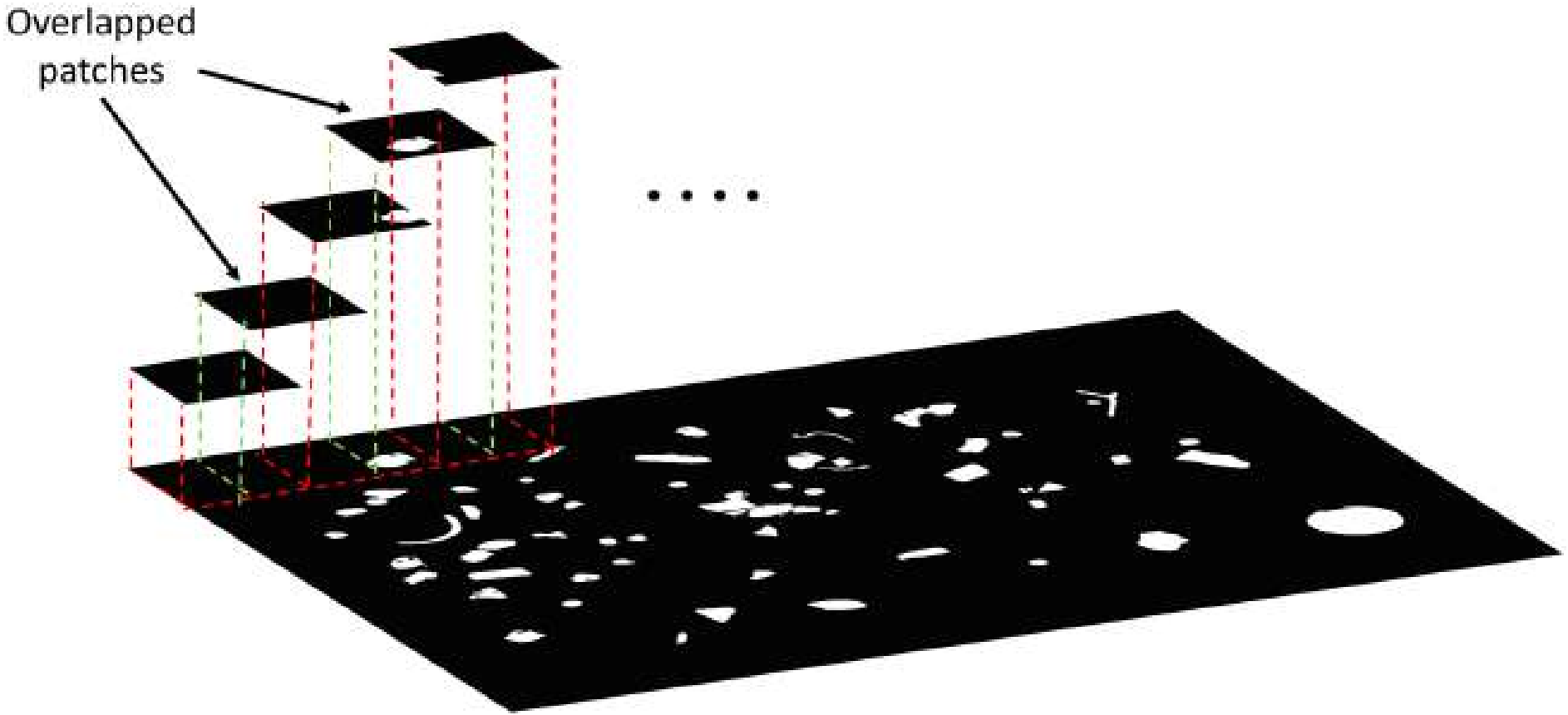

Figure 4

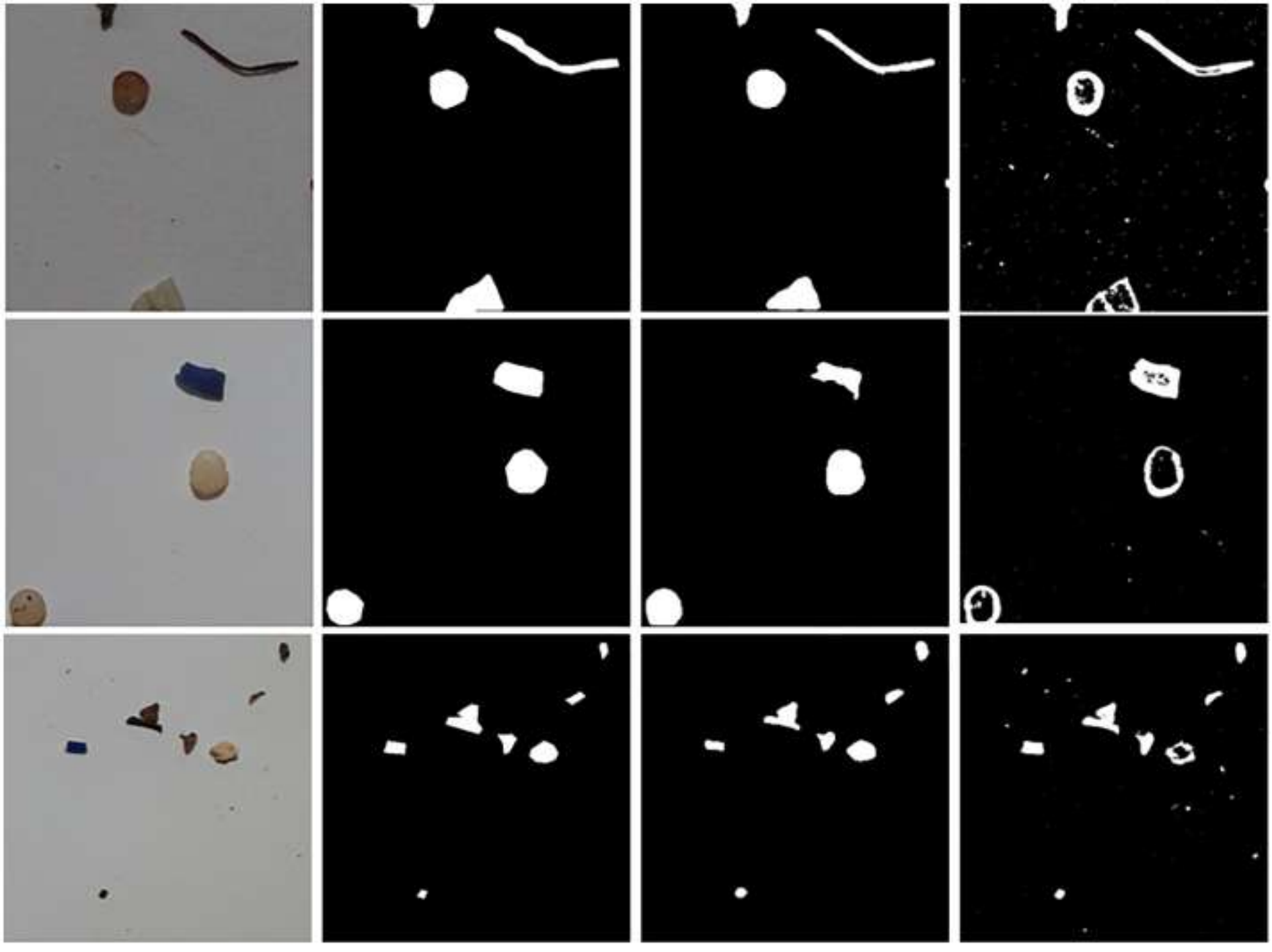

Figure 5

Real: Fragment
Predicted: Pellet

Real: Pellet
Predicted: Fragment

Real: Pellet
Predicted: Fragment

Real: Pellet
Predicted: Fragment

Figure 6

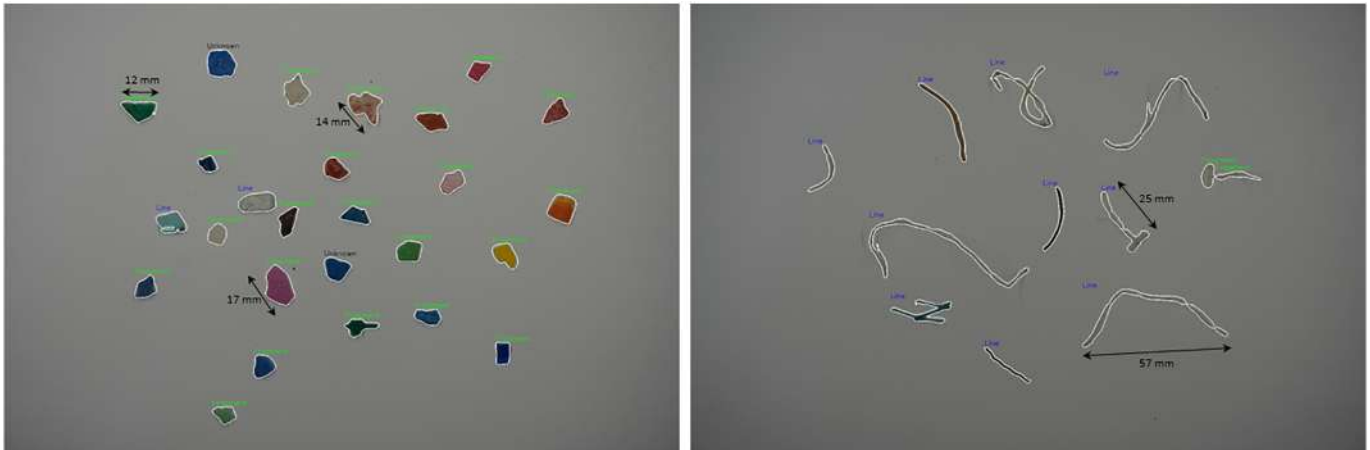

(a) (b)

Figure 7